Mutations in *C11orf70* Cause Primary Ciliary Dyskinesia with Randomization of Left/Right Body Asymmetry Due to Defects of Outer and Inner Dynein Arms

Inga M. Höben,[1] Rim Hjeij,[1] Heike Olbrich,[1] Gerard W. Dougherty,[1] Tabea Nöthe-Menchen,[1] Isabella Aprea,[1] Diana Frank,[1] Petra Pennekamp,[1] Bernd Dworniczak,[1] Julia Wallmeier,[1] Johanna Raidt,[1] Kim G. Nielsen,[2] Maria C. Philipsen,[2] Francesca Santamaria,[3] Laura Venditto,[3] Israel Amirav,[4] Huda Mussaffi,[5,6] Freerk Prenzel,[7] Kaman Wu,[8] Zeineb Bakey,[8] Miriam Schmidts,[8,9] Niki T. Loges,[1,10] and Heymut Omran[1,10,*]

Primary ciliary dyskinesia (PCD) is characterized by chronic airway disease, male infertility, and randomization of the left/right body axis as a result of defects of motile cilia and sperm flagella. We identified loss-of-function mutations in the open-reading frame *C11orf70* in PCD individuals from five distinct families. Transmission electron microscopy analyses and high-resolution immunofluorescence microscopy demonstrate that loss-of-function mutations in *C11orf70* cause immotility of respiratory cilia and sperm flagella, respectively, as a result of the loss of axonemal outer (ODAs) and inner dynein arms (IDAs), indicating that C11orf70 is involved in cytoplasmic assembly of dynein arms. Expression analyses of *C11orf70* showed that *C11orf70* is expressed in ciliated respiratory cells and that the expression of *C11orf70* is upregulated during ciliogenesis, similar to other previously described cytoplasmic dynein-arm assembly factors. Furthermore, C11orf70 shows an interaction with cytoplasmic ODA/IDA assembly factor DNAAF2, supporting our hypothesis that C11orf70 is a preassembly factor involved in the pathogenesis of PCD. The identification of additional genetic defects that cause PCD and male infertility is of great importance for the clinic as well as for genetic counselling.

Cilia are hair-like organelles extending from nearly all types of polarized cells. Motile cilia in distinct cell types in the human body perform essential biological functions such as generation of fluid flow and mucociliary clearance of the airways.[1] The basic structure of motile cilia consists of a ring of nine peripheral microtubule doublets, which surround one central pair (9 + 2 structure). The peripheral ring is connected to the central pair (CP) through radial spokes (RSs) and the nexin-dynein regulatory complex (N-DRC). The CP, the N-DRC, and the inner dynein arms (IDAs) are responsible for modulation and regulation of the ciliary beating[2,3] whereas the outer dynein arms (ODAs) are responsible for the beat generation. ODAs and IDAs are large multimeric protein complexes that are pre-assembled in the cytoplasm before transport to the axonemes.[4] There are at least two types of ODAs in humans: type 1, containing the axonemal dynein heavy chains (HCs) DNAH5 and DNAH11, located proximally, and type 2, containing the dynein HCs DNAH5 and DNAH9, located distally in the ciliary axonemes.[5,6] In *Chlamydomonas reinhardtii*, there are seven distinct IDA complexes, one double-headed and six single-headed.[7] The IDA I1 complex contains two HCs (α- and β-HC) and the intermediate-chain light-chain complex (ICLC).[8] The six single-headed complexes can be divided into two groups on the basis of their association with specific light chains: the three IDA complexes of group I2 contain each one HC that associates with the dynein light chain p28.[7] The IDA complexes of group I3 also each contain one HC, which associates with centrin.[7] The identification of proteins responsible for the correct assembly and composition of these protein complexes is critical to understanding the disease mechanisms of motile-cilia-related disorders such as primary ciliary dyskinesia (PCD).

Primary ciliary dykinesia (PCD) (MIM: 244400) is a rare genetic disorder caused by immotile or dyskinetic cilia and has a prevalence in the range of 1:4.000 to 1:20.000.[9] Ciliary dysfunction in upper and lower airways leads to defective mucociliary clearance of the airways and subsequently to recurrent airway inflammation, bronchiectasis (Figure 1), and progressive lung failure. Dysfunction of cilia of the left-right organizer (LRO) during early embryonic development results in randomization of the left/right body asymmetry. Approximately half of the PCD individuals exhibit *situs inversus totalis* (Figure 1), referred to as Kartagener's syndrome.[9] More rarely, other situs anomalies associated with complex congenital heart disease are observed.[10] Defects underlying motile-cilia

[1]Department of General Pediatrics, University Children's Hospital Muenster, 48149 Muenster, Germany; [2]Danish PCD Centre, Pediatrics Pulmonary Service, Department of Pediatrics and Adolescent Medicine, Copenhagen University Hospital, Rigshospitalet, 2100 Copenhagen, Denmark; [3]Department of Translational Medical Sciences, Federico II University, 80131 Naples, Italy; [4]Department of Pediatrics, University of Alberta, T6G 1C9 Edmonton, Alberta, Canada; [5]Schneider Children's Medical Center, 4920235 Petach-Tikva, Israel; [6]Sackler Faculty of Medicine, Tel Aviv University, Ramat Aviv, 69978 Tel Aviv, Israel; [7]Clinic for Pediatrics and Adolescent Medicine, University Hospital Leipzig, 04103 Leipzig, Germany; [8]Genome Research Division, Human Genetics Department, Radboud University Medical Center and Radboud Institute for Molecular Life Sciences, Geert Grooteplein Zuid 10, 6525KL Nijmegen, The Netherlands; [9]Pediatric Genetics Division, Center for Pediatrics and Adolescent Medicine, Faculty of Medicine, Freiburg University, Mathildenstrasse 1, 79112 Freiburg, Germany
[10]These authors contributed equally to this work
*Correspondence: heymut.omran@ukmuenster.de
https://doi.org/10.1016/j.ajhg.2018.03.025.

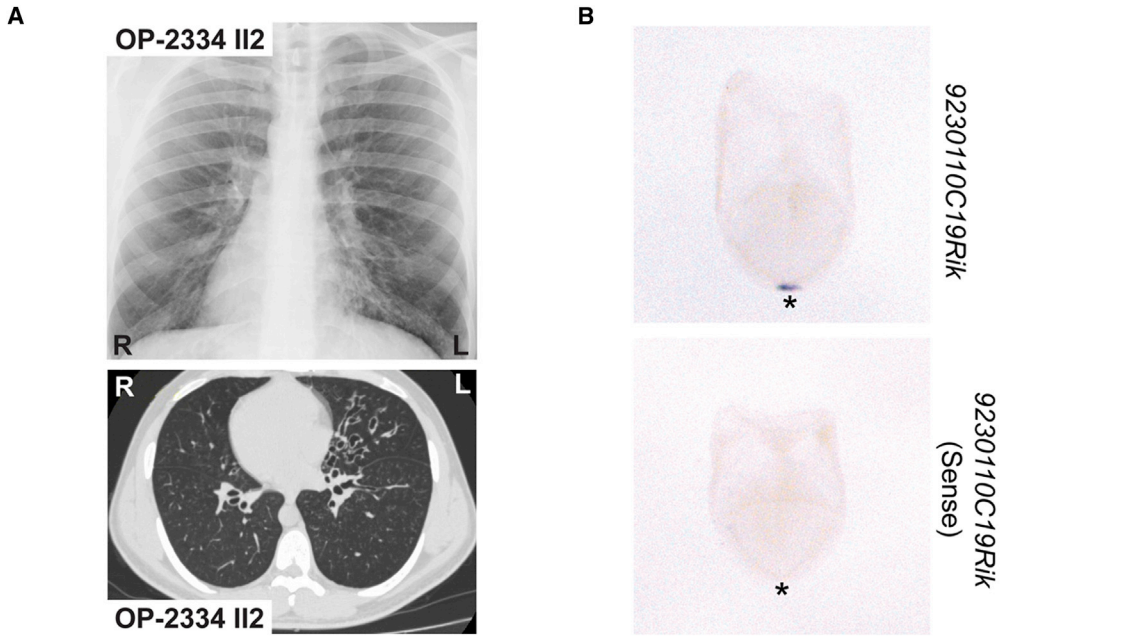

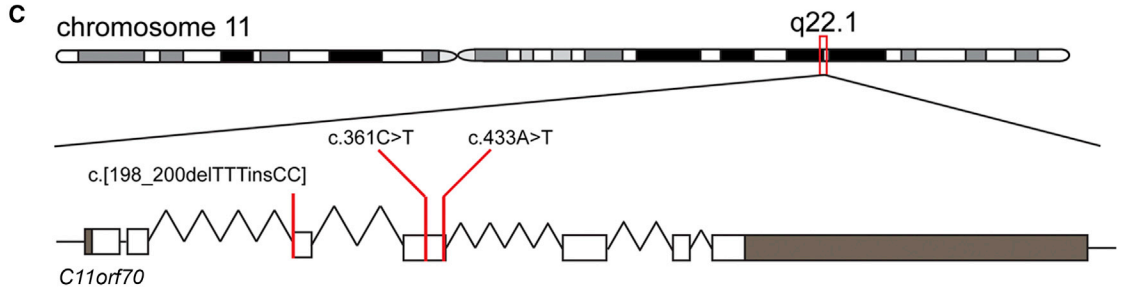

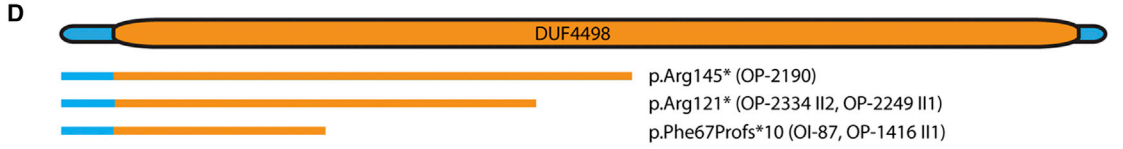

E

		Experiment #1						Experiment #2					
		Nasal biopsy			Blood			ALI-culture		Nasal biopsy		EBV cells	
	Sample	1	2	3	1	2	3	4	5	4	5	4	5
Gene	*CFAP161*	23	18	30	1	0	0	12	70	32	44	0	0
	DNAAF1	75	149	149	0	0	0	22	136	133	197	0	0
	DNAAF2	12	8	9	1	1	2	19	50	17	26	1	0
	DNAAF3	42	66	87	0	0	0	32	176	123	132	0	0
	DNAAF4	35	32	55	1	0	0	21	87	104	121	0	0
	DNAAF5	36	33	53	17	10	8	64	139	72	93	20	9
	LRRC6	27	28	39	7	1	4	10	80	61	96	0	0
	PIH1D3	11	8	13	0	0	0	6	36	32	44	0	0
	SPAG1	50	41	73	1	1	2	35	117	65	104	1	0
	ZMYND10	247	264	330	4	3	1	182	581	550	646	0	0
	C21orf59	105	84	163	11	8	10	125	213	352	265	13	6
	C11orf70	68	51	96	0	0	0	50	213	134	163	0	0
	GAPDH	1368	834	1241	1393	2062	3423	4256	2502	7133	1929	12375	7273

Figure 1. Recessive Loss-of-Function Mutations in *C11orf70* Cause Primary Ciliary Dyskinesia with Randomization of Left/Right Body Asymmetry

(A) The chest X-ray radiograph of PCD-affected individual OP-2334 II2 depicts *situs inversus totalis*. The computed tomography scan of OP-2334 II2 shows chronic airway disease with bronchiectasis in the middle lobe and mucus plugging.

(B) *In situ* hybridization analyses of wild-type 8.25 dpc (days post-coitum) mouse embryos reveal expression of *9230110C19Rik* (*C11orf70* ortholog) exclusively at the left/right organizer (frontal view; asterisks in the ventral position of the left/right organizer). By contrast, the negative control utilizing the sense probe does not show any staining.

(legend continued on next page)

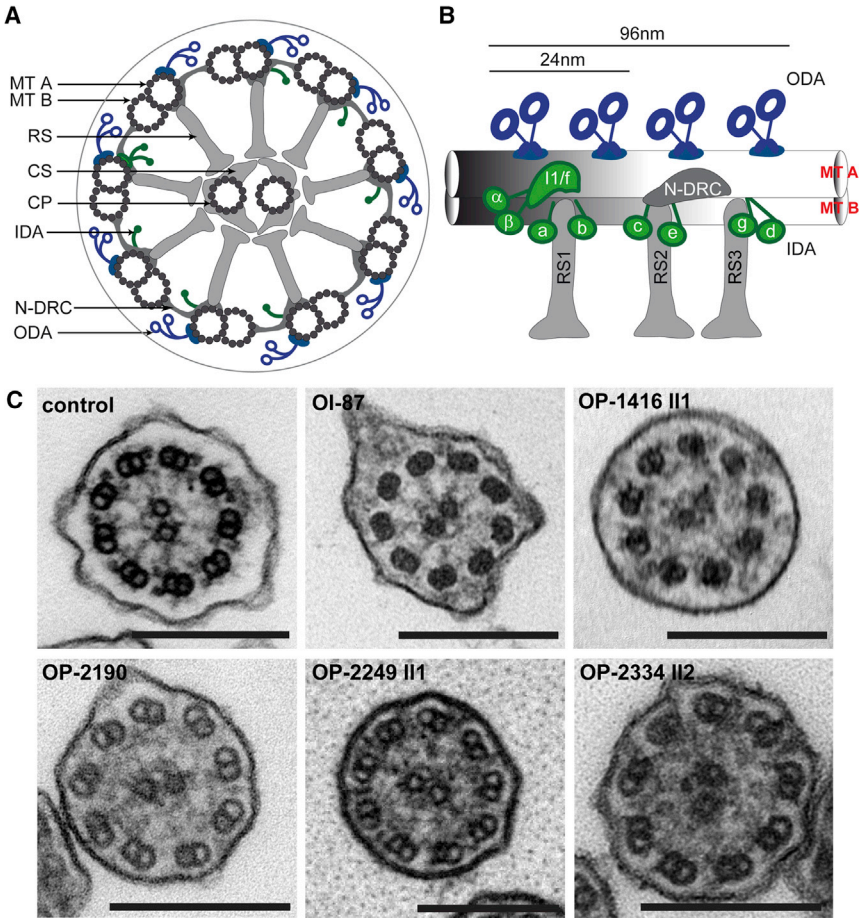

Figure 2. *C11orf70*-Mutant Respiratory Ciliary Axonemes Exhibit Ultrastructural Defects of the Outer and Inner Dynein Arms

(A) Schematic diagram of a cross-section through a motile respiratory 9 + 2 cilium.

(B) Arrangement of ODAs (blue) and IDAs (green) within the 96 nm unit in human ciliary axonemes. Whereas ODAs occur once every 24 nm within the 96 nm unit, the double-headed IDA complex I1/f, which contains the α- and β-heavy chain and the single-headed complexes (containing the dyneins a–d and g) are distributed with a 96 nm periodicity.

(C) Transmission electron-microscopy photographs of cross-sections through respiratory epithelial cilia demonstrate the absence of ODAs and IDAs in PCD-affected individuals OI-87, OP-1416 II1, OP-2190, OP-2249 II1, and OP-2334 II2 carrying biallelic *C11orf70* mutations, which was in contrast to a control cilium. The scale bar represents 200 nm. Abbreviations are as follows: CP, central pair; CS, central sheath; IDA, inner dynein arm; MT A, microtubule A; MT B, microtubule B; N-DRC, nexin-dynein regulatory complex; ODA, outer dynein arm; and RS, radial spoke.

dysfunction often affect sperm flagella function and cause male infertility in PCD-affected individuals, warranting assisted-reproductive technologies. Another consequence of ciliary dysfunction, particularly evident in PCD mouse models, is hydrocephalus formation caused by disrupted flow of the cerebrospinal fluid through the cerebral aqueduct connecting the third and fourth brain ventricles.[11] Although dysmotility of the ependymal cilia is not sufficient for hydrocephalus formation in humans, probably because of morphological differences between the mouse and human brain, the incidence of hydrocephalus, secondary to aqueduct closure, is increased in PCD-affected individuals.[11] PCD diagnosis is difficult and relies on a combination of tests, including nasal nitric oxide (nNO) production rate measurement, high-speed video-microscopy of cilia, ciliary-structure analyses by transmission electron microscopy (TEM),[12] and high-resolution immunofluorescence microscopy.

Until now, mutations in 39 genes, responsible for an estimated 70% of cases, have been linked to PCD.[13] Genetic analyses of PCD-affected individuals identified several autosomal-recessive mutations in genes encoding axonemal subunits of the ODA and ODA-docking complexes,[14–26] the N-DRC,[27–30] the 96 nm axonemal ruler proteins,[31,32] the RS,[33–36] and CP-associated proteins[13,37] (Figure 2). Although the process of cytoplasmic pre-assembly of dynein arms is still poorly understood, several genes encoding proteins involved in this process were identified: *DNAAF1* (*LRRC50*) (MIM: 613190),[38,39] *DNAAF2* (*KTU*) (MIM: 612517),[40] *DNAAF3* (*C19orf51*) (MIM: 614566),[41] *DNAAF4* (*DYX1C1*) (MIM: 608709),[42] *DNAAF5* (*HEATR2*) (MIM: 614864),[43] *LRRC6* (MIM: 614930),[44] *ZMYND10* (MIM: 607070),[45,46] *SPAG1* (MIM: 603395)[47] and *C21orf59* (MIM: 615494).[28] Three X-linked PCD variants have been reported so far: one caused by *PIH1D3* (MIM: 300933) mutations[48,49] resulting in the absence of ODA

(C) Schematic presentation of chromosome 11 and the exon-intron structure of *C11orf70* with untranslated (gray) and translated (white) regions. The positions of the three identified mutations in the five unrelated families are indicated by red lines.

(D) Protein model of C11orf70 with the domain of unknown function 4498 (DUF 4498) and the predicted truncated proteins as consequences of the three *C11orf70* loss-of-function mutations.

(E) Differentiation-specific and tissue-specific expression profiles of known genes encoding proteins involved in outer- and inner-dynein-arm assembly and *GAPDH* as a housekeeping gene. Raw RNA-seq data were normalized against *PPIH* (*peptidylprolyl isomerase H*). The preassembly-factor genes have the strongest expression in native material of nasal-brushing biopsies. Comparable expression profiles are observed in ALI-cultured nasal epithelial cells and in nasal-brushing biopsies. EBV cells (immortalized lymphocytes) and blood cells show no or weak expression of genes encoding cytoplasmic dynein assembly factors. *GAPDH* shows a high expression in all analyzed tissues. We performed two independent experiments with samples from five control individuals (samples 1–5).

Table 1. Clinical Findings of PCD-Affected Individuals with Mutations in *C11orf70*

Subject	Sex	Origin	SI	nNo [nl/min]	Neonatal RDS	Recurrent Pneumonia	Recurrent Respiratory Infections	Bronchiectasis	Chronic Wet Cough	Otitis Media	Hearing Disorder	HVMA	Congenital Heart Defect	Fertility Defect
OI-87	F	Israel	no	26	yes	yes	yes	yes	yes	yes	yes	n.a.	no	probably (one child after IVF)
OP-1416 II1	F	Germany	no	13.3	yes	yes	yes	yes	n.a.	n.a.	yes	immotile	no	probably
OP-2190	F	Germany	no	5	yes	n.a.	yes	yes	yes	yes	n.a.	n.a.	no	n.a.
OP-2249 II1	F	Turkey	no	5.7	no	n.a.	yes	yes	yes	yes	n.a.	immotile	no	n.a.
OP-2334 II2	M	Italy	yes	28	no	yes	yes	yes	yes	yes	yes	immotile	no	yes

Abbreviations: F, female; M, male; SI, *situs inversus*; nNO, nasal nitric oxide; RDS, respiratory distress syndrome; HVMA, high-speed video microscopy analyses; n.a., not available; and IVF, *in vitro* fertilization.

and IDA and two PCD variants caused by mutations in *OFD1* (MIM: 311200) and *RPGR* (MIM: 312610), which are associated with syndromic cognitive dysfunction or retinal degeneration, respectively.[50,51] Here, we describe an ODA/IDA defect caused by recessive loss-of-function mutations in the open-reading frame *C11orf70*.

We performed targeted-exome sequencing in 15 PCD-affected individuals with combined ODA and IDA defects of unknown genetic cause. Signed and informed consent was obtained from individuals fulfilling diagnostic criteria of PCD[12] and from family members according to protocols approved by the institutional ethics review board at the University of Muenster. Genomic DNA was isolated by standard methods directly from blood samples. Targeted-exome sequencing of genomic DNA was performed at the Cologne Center for Genomics. For enrichment, the NimbleGen SeqCap EZ Human Exome Library v2.0 was used. Enriched preparations were sequenced with the HiSeq2000 platform (Illumina) as paired-end 2 × 100 bp reads. The 30× coverage was in the range of 79%–86%. The genome sequence hg38 was used as a reference for mapping sequencing reads that passed quality filtering. Variants that were present in the dbSNP database, the 1000 Genomes Project polymorphism, and the Genome Aggregation Database (gnomAD) with a minor-allele frequency >0.01 were excluded. We focused on nonsynonymous mutations, splice-site substitutions, and indels following an autosomal-recessive inheritance pattern. In five PCD-affected individuals, we identified loss-of-function mutations in the chromosome 11 open-reading frame 70 (*C11orf70*) (GenBank: NM_032930.2). In OP-1416 II1 and OI-87, we identified a homozygous deletion of three thymine residues and an insertion of two cytosine residues (c.198_200delinsCC) resulting in a frameshift and predicted premature stop of translation (p.Phe67Profs*10; Figure 1 and Figure S1). In OP-2249 II1 and OP-2334 II2, we identified a transition from C>T at position 361 (c.361C>T), and in OP-2190 a transversion from A>T at position 433 (c.433A>T), both resulting in stop codons (p.Arg121* and p.Arg145*; Figure 1 and Figure S1).

All individuals with loss-of-function mutations in *C11orf70* show classical PCD symptoms (Table 1) such as chronic sinusitis, chronic otitis media, and chronic lower-respiratory-tract infections, as well as bronchiectasis in the middle lobe and mucus plugging (shown for OP-2334 II2 in Figure 1). Three of the five affected individuals had neonatal respiratory distress syndrome. In addition, one individual had *situs inversus totalis*, consistent with randomization of left/right body asymmetry (Figure 1). One individual underwent lobectomy of the middel lobe, because of recurrent exacerbations and frequent hemoptysis. The nasal nitric oxide production rate measured with the Niox Mino (Aerocrine) or EcoMedics CLD88 (EcoMedics) was low in all affected individuals (Table 1). High-speed video microscopy of ciliary motility in nasal respiratory epithelial cells showed completely immotile cilia (Videos

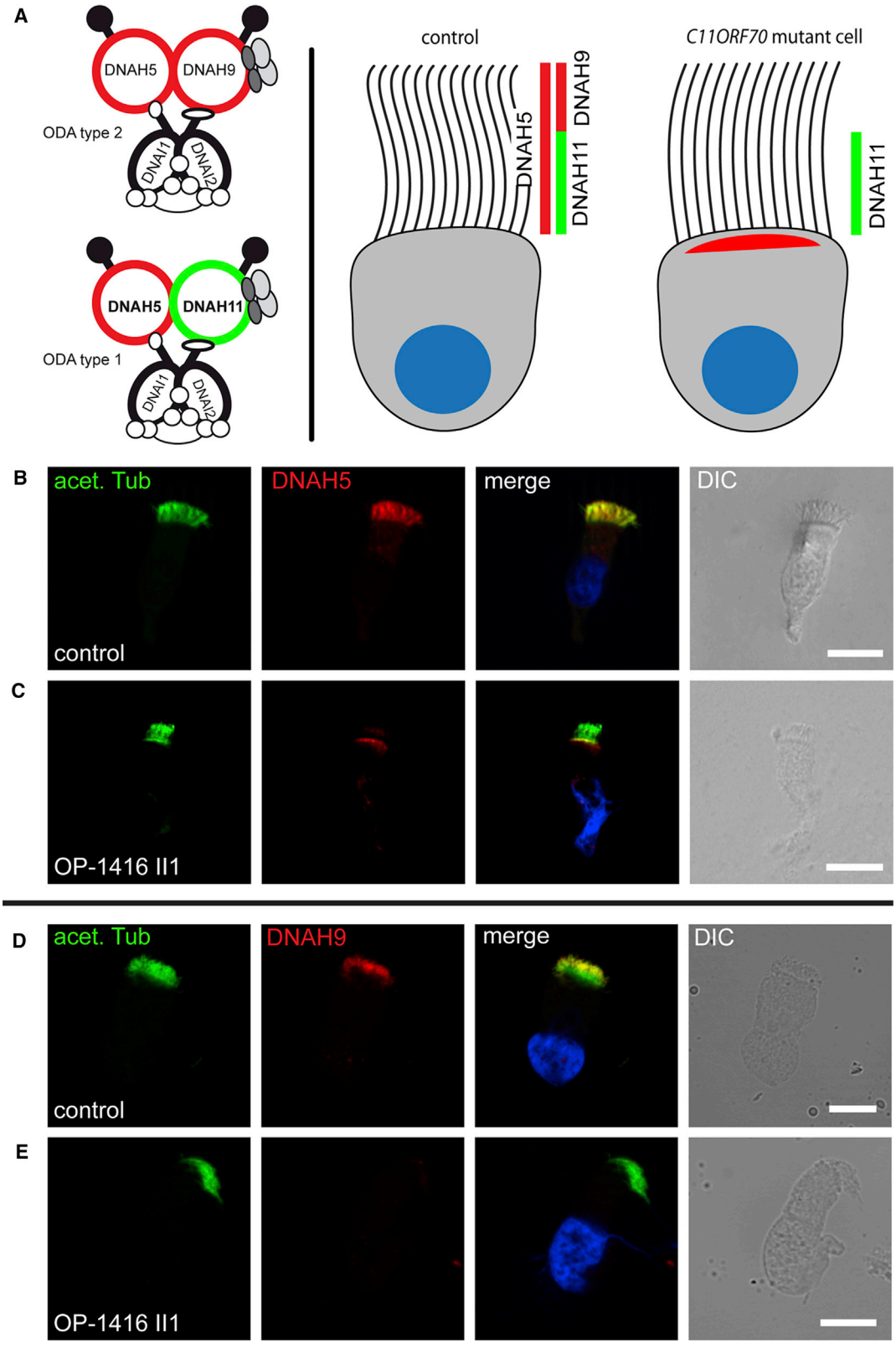

Figure 3. Absence of the Outer-Dynein-Arm Heavy Chains DNAH5 and DNAH9 in Respiratory Cilia of PCD-Affected Individuals Carrying *C11orf70* Mutations

(A) Schematics of type 1 and 2 ODAs show that DNAH11 is a component of type 1 ODA and localizes only to the proximal part, whereas DNAH9 is a component of type 2 ODA and localizes only to the distal part of the ciliary axonemes. DNAH5 is a component of both ODA types and localizes throughout the ciliary axoneme. In *C11orf70*-mutant cilia, DNAH5 and DNAH9 are absent from the ciliary axonemes, whereas DNAH11 localization is not affected by mutations in *C11orf70* (Figure S8).

(legend continued on next page)

S1, S2, and S3) in contrast to control cilia (Video S4). Ciliary-beat frequency and beating pattern was assessed with the SAVA system.[52] Respiratory epithelial cells were analyzed with a Zeiss AxioVert A1 microscope (40× and 63× phase-contrast objective lens) equipped with a Basler sc640-120fm monochrome high-speed video camera (Basler) set at 120 frames per second. The ciliary beating pattern was evaluated on slow-motion playbacks. Two individuals (OI-87 and OP-2334 II2) reported fertility problems. OI-87 gave birth to one child after *in vitro* fertilization. OP-2334 II2 had undergone fertility testing in the past and was diagnosed with moderate oligozoospermia (reduced number of sperm) and severe asthenozoospermia (immotility of sperm flagella) (Table S1). TEM analyses of respiratory cilia isolated from individuals with biallelic *C11orf70* mutations and sperm flagella from OP-2334 II2 displayed both ODA and IDA defects in all cases (Figure 2). We analyzed sperm flagella from OP-2334 II2 by high-speed video microscopy, and in contrast to control cells (Video S5), sperm cells from OP-2334 II2 were completely immotile (Videos S6 and S7), consistent with a loss of dynein arms. TEM of human respiratory cilia and sperm flagella was performed as previously described.[37]

Next, we analyzed *C11orf70* expression in various tissues to test whether the expression is consistent with function in motile cilia and the observed clinical phenotype. Therefore, we studied tissue-specific expression of *C11orf70* in Epstein Barr Virus (EBV)-transformed lymphocytes, nasal brushing biopsies, and respiratory cells grown on air liquid interface (ALI) culture to full differentiation, each obtained from healthy controls. ALI-cell culture and transformation of lymphocytes with EBVs were performed as previously described.[53,54] Human transcriptome profiles were generated by next-generation sequencing. RNA from nasal epithelial cells, ALI-cultured epithelial cells, and EBV-transformed lymphocytes were isolated with the RNeasy Mini Kit. RNA from blood samples was isolated with PAXgene Blood RNA (PreAnalytiX by QIAGEN). DNA contaminations were eliminated via TURBO DNA-*free* (Ambion by Life Technologies, Thermo Fisher). RNA quality and quantity were measured with the 2200 TapeStation (Agilent Technologies) and Qubit 3.0 Fluorometer (Thermo Fisher), and only RNA samples showing a RINe value of 8.0 or higher were used for RNA-seq. For the library construction, Ion AmpliSeq Library Plus Kit 2.0 (Thermo Fisher) and IonXpress Barcode Adaptor 1-96 (Thermo Fisher) were used. The Amplicon library preparation was carried out with an Ion-AmpliSeq Transcriptome Gene Expression Core Panel (20.000 genes in total, Thermo Fisher). The library pool for one RNA-seq approach with a maximum number of six samples was diluted to a final concentration of 20 pM with low-TE buffer. For the preparation of next-generation sequencing, IonSphere positive particles were generated via Emulsion PCR with the IonOneTouch System 2 (Thermo Fisher). Positive particles were enriched with Dynabeads MyOne Streptavidin C1 Beads (Thermo Fisher) and purified with the IonOneTouch Wash Solution Kit as well as the IonOneTouch ES module (Thermo Fisher). Prepared IonSphere positive particles were loaded into an Ion 318 Chip (Thermo Fisher) and sequenced with the Ion Proton platform for next-generation sequencing. Sequenced amplicons were aligned against the reference transcriptome hg19_AMpliSeq_Transcriptome_ERCC_v1.fastq (see Web Resources). Output data of a small selection of genes were normalized against the gene *peptidylprolyl isomerase H* (*PPIH*). Mutations in genes encoding dynein axonemal assembly factors (DNAAFs) result in combined ODA and IDA defects; these observations resemble those in *C11orf70* mutant cilia. Similar to known genes encoding cytoplasmic dynein preassembly factors, *C11orf70* was most strongly expressed in native material of biopsies obtained from nasal brushing. Comparable expression was observed in nasal-brushing biopsies and ALI-cultured nasal epithelial cells, whereas EBV-infected lymphocytes and blood cells usually showed no or weak expression levels (Figure 1). Interestingly, similar to the expression of genes encoding DNAAFs involved in ODA/IDA assembly (Figure S2), expression of *C11orf70* was upregulated during ciliogenesis between days 3 and 15. To determine whether loss of *C11orf70* function could explain the *situs* abnormalities observed in one of the investigated PCD-affected individuals with biallelic mutations, we performed *in situ* hybridization analyses of gastrulating mouse embryos during the developmental period when the LRO is present and body laterality is determined. *In situ* hybridization was performed as previously described.[42] A 619 bp fragment of *9230110C19Rik*/*C11orf70* (RefSeq: NM_199017.2) cDNA was amplified from wild-type mouse testis cDNA and subsequently ligated into pCRII-TOPO vector by a TOPO cloning reaction (Invitrogen, Thermo Fisher Scientific). We detected expression of *9230110C19Rik*/*C11orf70* during this essential developmental stage. Interestingly, the expression was restricted exclusively to the left/right organizer (Figure 1 and Figure S3). This finding strongly indicates that C11orf70 is involved in the function of motile nodal monocilia and that deficiency of this protein probably

(B and C) Respiratory cilia double-labeled with antibodies directed against acetylated α-tubulin (green) and DNAH5 (red) show colocalization of DNAH5 with acetylated α-tubulin along the cilia from unaffected controls (B, yellow). In contrast, DNAH5 is absent or severely reduced in *C11orf70*-mutant axonemes (C, shown for OP-1416 II1). Please note that the red signal at the ciliary base in (C) is an unspecific additional staining caused by rabbit polyclonal antibodies (see References[55] for further details).
(D and E) Respiratory epithelial cells from control and PCD-affected individuals were double-labeled with antibodies directed against acetylated tubulin (green) and DNAH9 (red). Acetylated α-tubulin localizes to the entire length of the ciliary axoneme, whereas DNAH9 localization is restricted to the distal part of the axoneme in healthy control cells (D). In *C11orf70*-mutant cells, DNAH9 is absent from the ciliary axonemes (E, shown for OP-1416 II1). Nuclei were stained with Hoechst33342 (blue). Scale bars represent 10 μm.

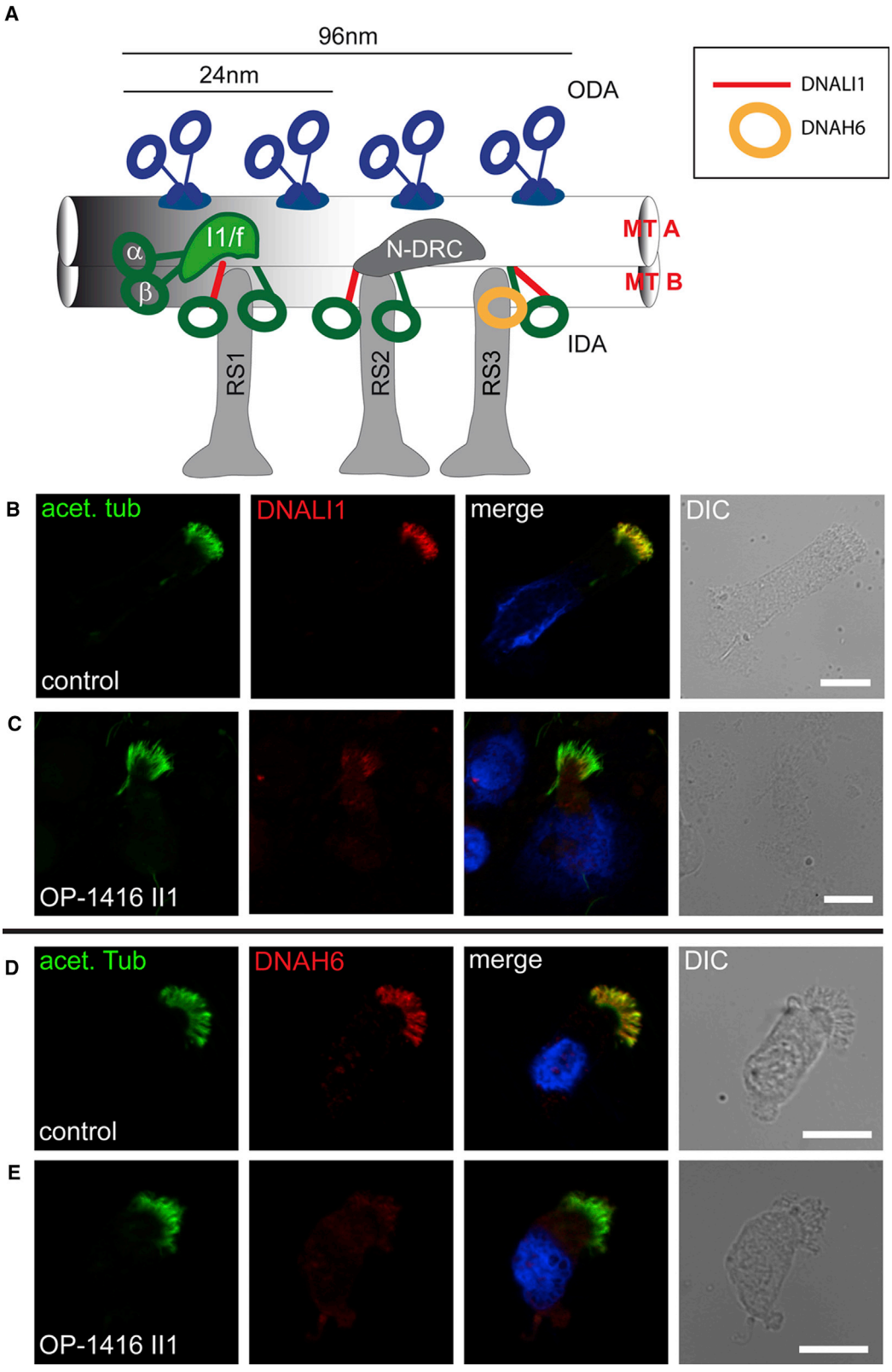

Figure 4. In *C11orf70*-Mutant Respiratory Cilia the IDA Light Chain DNALI1 (IDA-group I2) as Well as the IDA Heavy Chain DNAH6 (IDA-group I3) Are Absent

(A) Schematic of the arrangement of ODAs (blue) and IDAs (green) within the 96 nm unit in the human ciliary axoneme. IDA complexes a, c, and d belong to the IDA group I2, characterized by the presence of the dynein light chain DNALI1 (red lines). IDA complex g contains the dynein heavy chain DNAH6 (yellow circle) and belongs to the IDA group I3.

(B and C) Respiratory cilia double labeled with antibodies directed against acetylated α-tubulin (green) and DNALI1 (red) show colocalization of DNALI1 with acetylated α-tubulin along the cilia from unaffected controls (B, yellow). In contrast, DNALI1 is absent

(legend continued on next page)

causes an impairment of nodal ciliary beating, resulting in randomization of the left/right body axis.

To further understand the defect at the molecular level, we performed high-resolution immunofluorescence (IF) microscopy of respiratory cilia by using antibodies targeting components of the ODAs (DNAH5, DNAH9, DNAH11, DNAI1, and DNAI2), IDAs (DNALI1, in IDA group I2, and DNAH6, in IDA group I3), and ODA docking complexes (TTC25). High-resolution IF was performed as previously described.[42,55] We previously showed that respiratory cilia contain two distinct ODA types: type 1, which contains the dynein heavy chains DNAH5 and DNAH11 (proximal ciliary axoneme), and type 2, which contains the dynein heavy chains DNAH5 and DNAH9 (distal ciliary axoneme) (Figure 3).[5,6] The ODA components DNAH5, DNAH9, DNAI1, and DNAI2 were absent or severely reduced from the respiratory ciliary axonemes of the affected individuals (Figure 3 and Figures S4– S7). Interestingly, DNAH11 localization at the proximal part of the axoneme was not altered in *C11orf70* mutant cilia (Figure S8). However, TTC25 localization along the ciliary axoneme was not altered (Figure S9), indicating that loss of function of *C11orf70* does not affect composition and assembly of the ODA docking complex. We next asked whether assembly of the IDAs is also disturbed by C11orf70 deficiency. We found that DNALI1 and DNAH6 were severely reduced or completely absent from the ciliary axonemes in these PCD-affected individuals (Figure 4 and Figures S10 and S11), indicating that C11orf70 is also involved in the assembly of the IDA groups I2 and I3. Because OP-2334 II2 was diagnosed with severe asthenozoospermia and TEM analyses demonstrated a combined ODA/IDA defect (Figure 5), we performed high-resolution IF of sperm flagella by using antibodies directed against DNAI1, DNAI2, and DNALI1. ODA components DNAI1 and DNAI2 as well as the IDA component DNALI1 were absent or severely reduced from flagellar axonemes (Figure 5), demonstrating that C11orf70 is also involved in the preassembly of ODAs and IDAs in sperm cells.

In order to understand C11orf70 function within the cytoplasmic dynein-arm assembly process and to investigate possible interactions with other proteins encoded by genes causing PCD, we next performed a yeast two-hybrid (Y2H) screen as previously described.[48] Using C11ORF70 as bait, we tested putative interactions with other known preassembly factors, ODA and IDA components, ODA-DC proteins, proteins assumed to be involved in dynein-arm transport (DAW1/WDR69, IFT46), and others (Table S2). We tested direct interaction between C11orf70 and possible interactors as previously described.[48] All cDNA clones were confirmed by sequence analysis and matched RefSeq gene accession numbers. The screen revealed possible direct interaction with two assembly factors, namely DNAAF2 and PIH1D3 as well as with IFT46 (Figure S12). Because PIH1D3 and IFT46 pBD clones were found to be autoactivating (data not shown), we excluded these as interactions and considered only DNAAF2 as interacting physically with C11orf70. To confirm these results, we performed co-immunoprecipitation (co-IP) as previously described.[48] Interestingly, C11orf70 was able to pull down DNAAF2 but no other cytoplasmic preassembly factors, such as CCDC103 and PIH1D3 or the interflagellar transport protein IFT46 (Figure S12), confirming the findings from the Y2H screen.

Here, we demonstrate that deficiency of *C11orf70* results in defects of ODAs and IDAs and ciliary immotiliy; consequently, this alters mucociliary clearance and causes PCD. In one male PCD-affected individual, we observed sperm immotility, which is caused by disrupted assembly of dynein arms in sperm flagella; this finding was similar to those observed in *DNAAF2/KTU* mutant individuals.[40]

In summary, we identify recessive loss-of-function mutations in the open-reading frame *C11orf70* in five PCD-affected individuals from five distinct families. Interestingly, high-resolution IF analyses showed that loss of C11orf70 results in the absence of the type 1 and 2 ODAs. However, the localization of the β-heavy chain DNAH11 was not affected. We have demonstrated that axonemal DNAH11 assembly is independent of other axonemal dynein heavy chains such as DNAH5 and DNAH9 and that the cytoplasmic preassembly of DNAH11 is not dependent on the function of DNAAFs, such as DNAAF1 and DNAAF2.[6] Here, we demonstrate that loss of function of *C11orf70* results not only in defects of the axonemal assembly of IDAs of group I2 (as shown by the axonemal absence of DNALI1) but also of IDAs of group I3 (as shown by the axonemal loss of DNAH6), indicating that C11orf70 is involved in the assembly of those two IDA groups. Additionally, we demonstrated that C11orf70 deficiency results in the male-infertility-associated absence of ODAs and IDAs in sperm flagella. Binary interaction with DNAAF2 indicates a critical role for C11orf70 within the dynein-arm assembly machinery. We were unable to determine the cellular localization of C11orf70 because the availability of specific antibodies was lacking. However, the observed defects of ODAs and IDAs resembles findings observed in ciliary axonemes from individuals harboring mutations in *DNAAF* genes such as *DNAAF1*[38,39] and *DNAAF3*.[41] Additionally, the direct interaction with DNAAF2 indicates

or severely reduced in *C11orf70*-mutant axonemes (C, OP-1416 II1). Please note that the red signal at the ciliary base in (C) is an unspecific additional staining caused by rabbit polyclonal antibodies (see References[55] for further details).
(D and E) Respiratory epithelial cells from control and PCD-affected individuals were double labeled with antibodies directed against acetylated α-tubulin (green) and DNAH6 (red). DNAH6 colocalizes with acetylated tubulin along the cilia from unaffected controls (D, yellow). In contrast, DNAH6 is absent or severely reduced in *C11orf70*-mutant axonemes (E, OP-1416 II1). Nuclei were stained with Hoechst33342 (blue). Scale bars represent 10 μm.

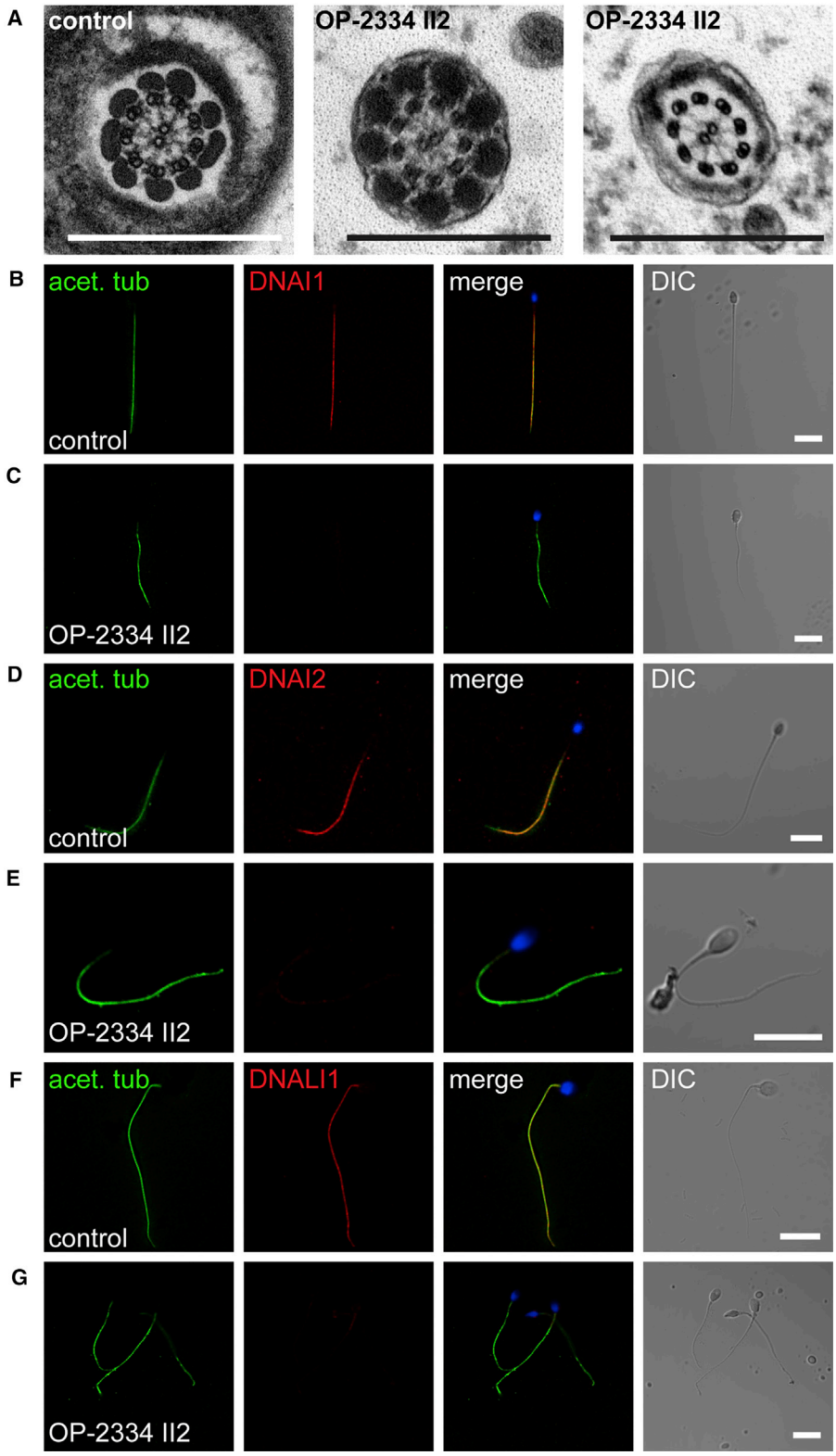

Figure 5. C11orf70 Is Necessary for Correct Assembly of Outer and Inner Dynein Arms in Sperm Flagella
(A) TEM photographs of cross-sections of sperm flagella from a healthy control individual and from OP-2334 II2. The outer and inner dynein arms are present in control sperm flagella but are absent from the sperm flagella of OP-2334 II2. The scale bar represents 500 nm. (B–G) To confirm the ultrastructural defects of the dynein arms, we double-labeled sperm from an unaffected control (B, D, and F) and OP-2334 II2 (C, E, and G) with antibodies directed against acetylated tubulin (green) and either ODA proteins (DNAI1 and DNAI2) or IDA protein (DNALI1) (red). DNAI1, DNAI2 and DNALI1 colocalize with acetylated tubulin along the sperm flagellum from the unaffected control (B, D, and F, yellow). In contrast, DNAI1, DNAI2, and DNALI1 are absent or severely reduced in *C11orf70*-mutant sperm flagella (C, E, and G). Nuclei were stained with Hoechst33342 (blue). Scale bars represent 10 μm.

that C11orf70 is probably a cytoplasmic preassembly factor and/or might be involved in the transport of dynein components to the ciliary axonemes.

Supplemental Data

Supplemental Data include twelve figures, two tables, and seven videos and can be found with this article online at https://doi.org/10.1016/j.ajhg.2018.03.025.

Acknowledgments

We are grateful to all affected individuals and their family members, whose cooperation made this study possible, and we thank all referring physicians. We thank A. Dorißen, D. Ernst, S. Helms, M. Herting, A. Robbers, L. Schwiddessen, F.J. Seesing, M. Tekaat, K. Wohlgemuth, and C. Westermann for excellent technical work. We would like to thank the Genome Aggregation Database and the groups that provided exome variant data for comparison. A full list of contributing groups can be found at http://gnomad.broadinstitute.org/. This work was supported by the Deutsche Forschungsgemeinschaft (DFG) OM6/7, OM6/8, OM6/9, OM6/10, OM6/11, and DFG KFO326 (H.O.), OL450/1 (H.Ol.), and HJ7/1-1 (R.H.), by the Interdisziplinäres Zentrum für Klinische Forschung (IZKF) Münster to H.O. (Om2/009/12 and Om/015/16), the European Union seventh framework program under grant agreement 305404, project BESTCILIA (to H.O., K.G.N., and M.C.P.) and "Innovative Medical Research" of the University of Muenster Medical School (I-LO121517 to N.T.L. and I-WA121418 to J.W.) and the Faculty of Medicine of the Westphalian Wilhelms University (to J.W.). M.S. acknowledges funding from Radboudumc and the Radboud Institute for Molecular Life Sciences Nijmegen (Hypatia tenure track fellowship), DFG (CRC1140 KIDGEM), and the European research Council (ERC StG TREATCilia, grant 716344). I.Am. acknowledges the Chief Office of the Ministry of Health in Israel grant number 3-6176.

Received: October 27, 2017
Accepted: March 23, 2018
Published: May 3, 2018

Web Resources

Ion AmpliSeq Designer, https://ampliseq.com
EMBL EBI Expression Atlas, http://www.ebi.ac.uk/gxa/home
Human Protein Atlas, http://www.proteinatlas.org/
Online Mendelian Inheritance in Man (OMIM), http://omim.org/
Varbank analysis software, https://varbank.ccg.uni-koeln.de/
Genome Aggregation Database (gnomAD), http://gnomad.broadinstitute.org

References

1. Fliegauf, M., Benzing, T., and Omran, H. (2007). When cilia go bad: Cilia defects and ciliopathies. Nat. Rev. Mol. Cell Biol. *8*, 880–893.
2. Satir, P. (1968). Studies on cilia. 3. Further studies on the cilium tip and a "sliding filament" model of ciliary motility. J. Cell Biol. *39*, 77–94.
3. Summers, K.E., and Gibbons, I.R. (1971). Adenosine triphosphate-induced sliding of tubules in trypsin-treated flagella of sea-urchin sperm. Proc. Natl. Acad. Sci. USA *68*, 3092–3096.
4. Fowkes, M.E., and Mitchell, D.R. (1998). The role of preassembled cytoplasmic complexes in assembly of flagellar dynein subunits. Mol. Biol. Cell *9*, 2337–2347.
5. Fliegauf, M., Olbrich, H., Horvath, J., Wildhaber, J.H., Zariwala, M.A., Kennedy, M., Knowles, M.R., and Omran, H. (2005). Mislocalization of DNAH5 and DNAH9 in respiratory cells from patients with primary ciliary dyskinesia. Am. J. Respir. Crit. Care Med. *171*, 1343–1349.
6. Dougherty, G.W., Loges, N.T., Klinkenbusch, J.A., Olbrich, H., Pennekamp, P., Menchen, T., Raidt, J., Wallmeier, J., Werner, C., Westermann, C., et al. (2016). DNAH11 localization in the proximal region of respiratory cilia defines distinct outer dynein arm complexes. Am. J. Respir. Cell Mol. Biol. *55*, 213–224.
7. Porter, M.E., and Sale, W.S. (2000). The 9 + 2 axoneme anchors multiple inner arm dyneins and a network of kinases and phosphatases that control motility. J. Cell Biol. *151*, F37–F42.
8. Heuser, T., Barber, C.F., Lin, J., Krell, J., Rebesco, M., Porter, M.E., and Nicastro, D. (2012). Cryoelectron tomography reveals doublet-specific structures and unique interactions in the I1 dynein. Proc. Natl. Acad. Sci. USA *109*, E2067–E2076.
9. Mirra, V., Werner, C., and Santamaria, F. (2017). Primary ciliary dyskinesia: An update on clinical aspects, genetics, diagnosis, and future treatment strategies. Front Pediatr. *5*, 135–147.
10. Kennedy, M.P., Omran, H., Leigh, M.W., Dell, S., Morgan, L., Molina, P.L., Robinson, B.V., Minnix, S.L., Olbrich, H., Severin, T., et al. (2007). Congenital heart disease and other heterotaxic defects in a large cohort of patients with primary ciliary dyskinesia. Circulation *115*, 2814–2821.
11. Ibañez-Tallon, I., Pagenstecher, A., Fliegauf, M., Olbrich, H., Kispert, A., Ketelsen, U.P., North, A., Heintz, N., and Omran, H. (2004). Dysfunction of axonemal dynein heavy chain Mdnah5 inhibits ependymal flow and reveals a novel mechanism for hydrocephalus formation. Hum. Mol. Genet. *13*, 2133–2141.
12. Lucas, J.S., Barbato, A., Collins, S.A., Goutaki, M., Behan, L., Caudri, D., Dell, S., Eber, E., Escudier, E., Hirst, R.A., et al. (2017). European Respiratory Society guidelines for the diagnosis of primary ciliary dyskinesia. Eur. Respir. J. *49*, 49.
13. Edelbusch, C., Cindrić, S., Dougherty, G.W., Loges, N.T., Olbrich, H., Rivlin, J., Wallmeier, J., Pennekamp, P., Amirav, I., and Omran, H. (2017). Mutation of serine/threonine protein kinase 36 (STK36) causes primary ciliary dyskinesia with a central pair defect. Hum. Mutat. *38*, 964–969.
14. Olbrich, H., Häffner, K., Kispert, A., Völkel, A., Volz, A., Sasmaz, G., Reinhardt, R., Hennig, S., Lehrach, H., Konietzko, N., et al. (2002). Mutations in DNAH5 cause primary ciliary dyskinesia and randomization of left-right asymmetry. Nat. Genet. *30*, 143–144.
15. Pennarun, G., Escudier, E., Chapelin, C., Bridoux, A.M., Cacheux, V., Roger, G., Clément, A., Goossens, M., Amselem, S., and Duriez, B. (1999). Loss-of-function mutations in a human gene related to Chlamydomonas reinhardtii dynein IC78 result in primary ciliary dyskinesia. Am. J. Hum. Genet. *65*, 1508–1519.
16. Panizzi, J.R., Becker-Heck, A., Castleman, V.H., Al-Mutairi, D., Liu, Y., Loges, N.T., Pathak, N., Austin-Tse, C., Sheridan, E., Schmidts, M., et al. (2012). CCDC103 mutations cause primary ciliary dyskinesia by disrupting assembly of ciliary dynein arms. Nat. Genet. *44*, 714–719.

17. Loges, N.T., Olbrich, H., Fenske, L., Mussaffi, H., Horvath, J., Fliegauf, M., Kuhl, H., Baktai, G., Peterffy, E., Chodhari, R., et al. (2008). DNAI2 mutations cause primary ciliary dyskinesia with defects in the outer dynein arm. Am. J. Hum. Genet. *83*, 547–558.
18. Mazor, M., Alkrinawi, S., Chalifa-Caspi, V., Manor, E., Sheffield, V.C., Aviram, M., and Parvari, R. (2011). Primary ciliary dyskinesia caused by homozygous mutation in DNAL1, encoding dynein light chain 1. Am. J. Hum. Genet. *88*, 599–607.
19. Duriez, B., Duquesnoy, P., Escudier, E., Bridoux, A.M., Escalier, D., Rayet, I., Marcos, E., Vojtek, A.M., Bercher, J.F., and Amselem, S. (2007). A common variant in combination with a nonsense mutation in a member of the thioredoxin family causes primary ciliary dyskinesia. Proc. Natl. Acad. Sci. USA *104*, 3336–3341.
20. Bartoloni, L., Blouin, J.L., Pan, Y., Gehrig, C., Maiti, A.K., Scamuffa, N., Rossier, C., Jorissen, M., Armengot, M., Meeks, M., et al. (2002). Mutations in the DNAH11 (axonemal heavy chain dynein type 11) gene cause one form of situs inversus totalis and most likely primary ciliary dyskinesia. Proc. Natl. Acad. Sci. USA *99*, 10282–10286.
21. Schwabe, G.C., Hoffmann, K., Loges, N.T., Birker, D., Rossier, C., de Santi, M.M., Olbrich, H., Fliegauf, M., Failly, M., Liebers, U., et al. (2008). Primary ciliary dyskinesia associated with normal axoneme ultrastructure is caused by DNAH11 mutations. Hum. Mutat. *29*, 289–298.
22. Knowles, M.R., Leigh, M.W., Carson, J.L., Davis, S.D., Dell, S.D., Ferkol, T.W., Olivier, K.N., Sagel, S.D., Rosenfeld, M., Burns, K.A., et al.; Genetic Disorders of Mucociliary Clearance Consortium (2012). Mutations of DNAH11 in patients with primary ciliary dyskinesia with normal ciliary ultrastructure. Thorax *67*, 433–441.
23. Hjeij, R., Lindstrand, A., Francis, R., Zariwala, M.A., Liu, X., Li, Y., Damerla, R., Dougherty, G.W., Abouhamed, M., Olbrich, H., et al. (2013). ARMC4 mutations cause primary ciliary dyskinesia with randomization of left/right body asymmetry. Am. J. Hum. Genet. *93*, 357–367.
24. Onoufriadis, A., Paff, T., Antony, D., Shoemark, A., Micha, D., Kuyt, B., Schmidts, M., Petridi, S., Dankert-Roelse, J.E., Haarman, E.G., et al.; UK10K (2013). Splice-site mutations in the axonemal outer dynein arm docking complex gene CCDC114 cause primary ciliary dyskinesia. Am. J. Hum. Genet. *92*, 88–98.
25. Knowles, M.R., Leigh, M.W., Ostrowski, L.E., Huang, L., Carson, J.L., Hazucha, M.J., Yin, W., Berg, J.S., Davis, S.D., Dell, S.D., et al.; Genetic Disorders of Mucociliary Clearance Consortium (2013). Exome sequencing identifies mutations in CCDC114 as a cause of primary ciliary dyskinesia. Am. J. Hum. Genet. *92*, 99–106.
26. Hjeij, R., Onoufriadis, A., Watson, C.M., Slagle, C.E., Klena, N.T., Dougherty, G.W., Kurkowiak, M., Loges, N.T., Diggle, C.P., Morante, N.F.C., et al.; UK10K Consortium (2014). CCDC151 mutations cause primary ciliary dyskinesia by disruption of the outer dynein arm docking complex formation. Am. J. Hum. Genet. *95*, 257–274.
27. Wirschell, M., Olbrich, H., Werner, C., Tritschler, D., Bower, R., Sale, W.S., Loges, N.T., Pennekamp, P., Lindberg, S., Stenram, U., et al. (2013). The nexin-dynein regulatory complex subunit DRC1 is essential for motile cilia function in algae and humans. Nat. Genet. *45*, 262–268.
28. Austin-Tse, C., Halbritter, J., Zariwala, M.A., Gilberti, R.M., Gee, H.Y., Hellman, N., Pathak, N., Liu, Y., Panizzi, J.R., Patel-King, R.S., et al. (2013). Zebrafish ciliopathy screen plus human mutational analysis identifies C21orf59 and CCDC65 defects as causing primary ciliary dyskinesia. Am. J. Hum. Genet. *93*, 672–686.
29. Horani, A., Brody, S.L., Ferkol, T.W., Shoseyov, D., Wasserman, M.G., Ta-shma, A., Wilson, K.S., Bayly, P.V., Amirav, I., Cohen-Cymberknoh, M., et al. (2013). CCDC65 mutation causes primary ciliary dyskinesia with normal ultrastructure and hyperkinetic cilia. PLoS ONE *8*, e72299.
30. Olbrich, H., Cremers, C., Loges, N.T., Werner, C., Nielsen, K.G., Marthin, J.K., Philipsen, M., Wallmeier, J., Pennekamp, P., Menchen, T., et al. (2015). Loss-of-function GAS8 mutations cause primary ciliary dyskinesia and disrupt the Nexin-Dynein regulatory complex. Am. J. Hum. Genet. *97*, 546–554.
31. Merveille, A.C., Davis, E.E., Becker-Heck, A., Legendre, M., Amirav, I., Bataille, G., Belmont, J., Beydon, N., Billen, F., Clément, A., et al. (2011). CCDC39 is required for assembly of inner dynein arms and the dynein regulatory complex and for normal ciliary motility in humans and dogs. Nat. Genet. *43*, 72–78.
32. Becker-Heck, A., Zohn, I.E., Okabe, N., Pollock, A., Lenhart, K.B., Sullivan-Brown, J., McSheene, J., Loges, N.T., Olbrich, H., Haeffner, K., et al. (2011). The coiled-coil domain containing protein CCDC40 is essential for motile cilia function and left-right axis formation. Nat. Genet. *43*, 79–84.
33. Castleman, V.H., Romio, L., Chodhari, R., Hirst, R.A., de Castro, S.C., Parker, K.A., Ybot-Gonzalez, P., Emes, R.D., Wilson, S.W., Wallis, C., et al. (2009). Mutations in radial spoke head protein genes RSPH9 and RSPH4A cause primary ciliary dyskinesia with central-microtubular-pair abnormalities. Am. J. Hum. Genet. *84*, 197–209.
34. Ziętkiewicz, E., Bukowy-Bieryłło, Z., Voelkel, K., Klimek, B., Dmeńska, H., Pogorzelski, A., Sulikowska-Rowińska, A., Rutkiewicz, E., and Witt, M. (2012). Mutations in radial spoke head genes and ultrastructural cilia defects in East-European cohort of primary ciliary dyskinesia patients. PLoS ONE *7*, e33667.
35. Frommer, A., Hjeij, R., Loges, N.T., Edelbusch, C., Jahnke, C., Raidt, J., Werner, C., Wallmeier, J., Große-Onnebrink, J., Olbrich, H., et al. (2015). Immunofluorescence analysis and diagnosis of primary ciliary dyskinesia with radial spoke defects. Am. J. Respir. Cell Mol. Biol. *53*, 563–573.
36. El Khouri, E., Thomas, L., Jeanson, L., Bequignon, E., Vallette, B., Duquesnoy, P., Montantin, G., Copin, B., Dastot-Le Moal, F., Blanchon, S., et al. (2016). Mutations in *DNAJB13*, encoding an HSP40 family member, cause primary ciliary dyskinesia and male infertility. Am. J. Hum. Genet. *99*, 489–500.
37. Olbrich, H., Schmidts, M., Werner, C., Onoufriadis, A., Loges, N.T., Raidt, J., Banki, N.F., Shoemark, A., Burgoyne, T., Al Turki, S., et al.; UK10K Consortium (2012). Recessive HYDIN mutations cause primary ciliary dyskinesia without randomization of left-right body asymmetry. Am. J. Hum. Genet. *91*, 672–684.
38. Loges, N.T., Olbrich, H., Becker-Heck, A., Häffner, K., Heer, A., Reinhard, C., Schmidts, M., Kispert, A., Zariwala, M.A., Leigh, M.W., et al. (2009). Deletions and point mutations of LRRC50 cause primary ciliary dyskinesia due to dynein arm defects. Am. J. Hum. Genet. *85*, 883–889.
39. Duquesnoy, P., Escudier, E., Vincensini, L., Freshour, J., Bridoux, A.-M., Coste, A., Deschildre, A., de Blic, J., Legendre, M., Montantin, G., et al. (2009). Loss-of-function mutations in the human ortholog of Chlamydomonas reinhardtii

ODA7 disrupt dynein arm assembly and cause primary ciliary dyskinesia. Am. J. Hum. Genet. *85*, 890–896.

40. Omran, H., Kobayashi, D., Olbrich, H., Tsukahara, T., Loges, N.T., Hagiwara, H., Zhang, Q., Leblond, G., O'Toole, E., Hara, C., et al. (2008). Ktu/PF13 is required for cytoplasmic pre-assembly of axonemal dyneins. Nature *456*, 611–616.
41. Mitchison, H.M., Schmidts, M., Loges, N.T., Freshour, J., Dritsoula, A., Hirst, R.A., O'Callaghan, C., Blau, H., Al Dabbagh, M., Olbrich, H., et al. (2012). Mutations in axonemal dynein assembly factor DNAAF3 cause primary ciliary dyskinesia. Nat. Genet. *44*, 381–389, S1–S2.
42. Tarkar, A., Loges, N.T., Slagle, C.E., Francis, R., Dougherty, G.W., Tamayo, J.V., Shook, B., Cantino, M., Schwartz, D., Jahnke, C., et al.; UK10K (2013). DYX1C1 is required for axonemal dynein assembly and ciliary motility. Nat. Genet. *45*, 995–1003.
43. Horani, A., Druley, T.E., Zariwala, M.A., Patel, A.C., Levinson, B.T., Van Arendonk, L.G., Thornton, K.C., Giacalone, J.C., Albee, A.J., Wilson, K.S., et al. (2012). Whole-exome capture and sequencing identifies HEATR2 mutation as a cause of primary ciliary dyskinesia. Am. J. Hum. Genet. *91*, 685–693.
44. Kott, E., Duquesnoy, P., Copin, B., Legendre, M., Dastot-Le Moal, F., Montantin, G., Jeanson, L., Tamalet, A., Papon, J.-F., Siffroi, J.-P., et al. (2012). Loss-of-function mutations in *LRRC6*, a gene essential for proper axonemal assembly of inner and outer dynein arms, cause primary ciliary dyskinesia. Am. J. Hum. Genet. *91*, 958–964.
45. Moore, D.J., Onoufriadis, A., Shoemark, A., Simpson, M.A., zur Lage, P.I., de Castro, S.C., Bartoloni, L., Gallone, G., Petridi, S., Woollard, W.J., et al. (2013). Mutations in *ZMYND10*, a gene essential for proper axonemal assembly of inner and outer dynein arms in humans and flies, cause primary ciliary dyskinesia. Am. J. Hum. Genet. *93*, 346–356.
46. Zariwala, M.A., Gee, H.Y., Kurkowiak, M., Al-Mutairi, D.A., Leigh, M.W., Hurd, T.W., Hjeij, R., Dell, S.D., Chaki, M., Dougherty, G.W., et al. (2013). *ZMYND10* is mutated in primary ciliary dyskinesia and interacts with LRRC6. Am. J. Hum. Genet. *93*, 336–345.
47. Knowles, M.R., Ostrowski, L.E., Loges, N.T., Hurd, T., Leigh, M.W., Huang, L., Wolf, W.E., Carson, J.L., Hazucha, M.J., Yin, W., et al. (2013). Mutations in *SPAG1* cause primary ciliary dyskinesia associated with defective outer and inner dynein arms. Am. J. Hum. Genet. *93*, 711–720.
48. Paff, T., Loges, N.T., Aprea, I., Wu, K., Bakey, Z., Haarman, E.G., Daniels, J.M.A., Sistermans, E.A., Bogunovic, N., Dougherty, G.W., et al. (2017). Mutations in *PIH1D3* cause X-linked primary ciliary dyskinesia with outer and inner dynein arm defects. Am. J. Hum. Genet. *100*, 160–168.
49. Olcese, C., Patel, M.P., Shoemark, A., Kiviluoto, S., Legendre, M., Williams, H.J., Vaughan, C.K., Hayward, J., Goldenberg, A., Emes, R.D., et al.; UK10K Rare Group (2017). X-linked primary ciliary dyskinesia due to mutations in the cytoplasmic axonemal dynein assembly factor PIH1D3. Nat. Commun. *8*, 14279.
50. Budny, B., Chen, W., Omran, H., Fliegauf, M., Tzschach, A., Wisniewska, M., Jensen, L.R., Raynaud, M., Shoichet, S.A., Badura, M., et al. (2006). A novel X-linked recessive mental retardation syndrome comprising macrocephaly and ciliary dysfunction is allelic to oral-facial-digital type I syndrome. Hum. Genet. *120*, 171–178.
51. Moore, A., Escudier, E., Roger, G., Tamalet, A., Pelosse, B., Marlin, S., Clément, A., Geremek, M., Delaisi, B., Bridoux, A.-M., et al. (2006). RPGR is mutated in patients with a complex X linked phenotype combining primary ciliary dyskinesia and retinitis pigmentosa. J. Med. Genet. *43*, 326–333.
52. Sisson, J.H., Stoner, J.A., Ammons, B.A., and Wyatt, T.A. (2003). All-digital image capture and whole-field analysis of ciliary beat frequency. J. Microsc. *211*, 103–111.
53. Munye, M.M., Shoemark, A., Hirst, R.A., Delhove, J.M., Sharp, T.V., McKay, T.R., O'Callaghan, C., Baines, D.L., Howe, S.J., and Hart, S.L. (2017). BMI-1 extends proliferative potential of human bronchial epithelial cells while retaining their mucociliary differentiation capacity. Am. J. Physiol. Lung Cell. Mol. Physiol. *312*, L258–L267.
54. Steel, C.M., Philipson, J., Arthur, E., Gardiner, S.E., Newton, M.S., and McIntosh, R.V. (1977). Possibility of EB virus preferentially transforming a subpopulation of human B lymphocytes. Nature *270*, 729–731.
55. Omran, H., and Loges, N.T. (2009). Immunofluorescence staining of ciliated respiratory epithelial cells. Methods Cell Biol. *91*, 123–133.